Structure sensitivity in the CO oxidation on rhodium: effect of adsorbate coverages on oxidation kinetics on Rh(100) and Rh(111)

Structure sensitivity in the CO oxidation on rhodium: Effect of adsorbate coverages on oxidation kinetics on Rh(100) and Rh(111)

M. J. P. Hopstaken and J. W. Niemantsverdriet[a)]
Schuit Institute of Catalysis, Eindhoven University of Technology, P.O. Box 513, 5600 MB Eindhoven, The Netherlands

(Received 14 April 2000; accepted 3 July 2000)

Temperature-programmed reaction spectroscopy has been used to study the surface reaction between CO and O-atoms on Rh(100) and Rh(111) at a range of different adsorbate coverages. Comparison of the reaction on both surfaces in the low coverage regime, where the kinetics can be described by a straightforward Langmuir–Hinshelwood mechanism reveals that the CO oxidation is structure sensitive, with the rate constant being an order of magnitude higher on the Rh(100) than on the Rh(111) surface. As a consequence, the selectivity of the CO+O reaction to CO_2 is about 100% on Rh(100), whereas on Rh(111) the oxidation reaction competes with CO desorption. At low CO coverage, CO oxidation is an elementary step on Rh(100) for a broad range of oxygen coverages. We report kinetic parameters $E_a = 103 \pm 5$ kJ/mol and $\nu = 10^{12.7 \pm 0.7}$ for $\theta_O = \theta_{CO} \rightarrow 0$ on Rh(100). The activation energy for CO oxidation on Rh(100) decreases continuously with increasing O-coverage. At low coverage ($\theta_O < 0.25$ ML) we attribute this to destabilization of CO, leading to an increase in the CO_2 formation rate. At higher coverage ($\theta_O > 0.25$ ML) O-atoms become destabilized as well, as lateral interactions between O-atoms come into play at these coverages. The interactions result in a greatly enhanced rate of reaction at higher coverages. © *2000 American Institute of Physics.* [S0021-9606(00)70237-6]

I. INTRODUCTION

The oxidation of CO on noble metals such as platinum,[1–3] rhodium,[4–20] palladium,[21–23] and ruthenium[6,21,24] is one of the most studied catalytic reactions in surface science. In the context of automotive exhaust catalysis the CO oxidation is important in two respects: first, in the reaction between O_2 and CO, which is most efficiently catalyzed by platinum and palladium, and second, in the removal of atomic oxygen originating from NO decomposition, for which rhodium and to a lesser extent palladium are the best catalysts. CO oxidation has been studied on different rhodium surfaces, e.g., Rh(111),[4–13] Rh(110),[11,14,15] Rh(100),[6,7,10,16–18] polycrystalline Rh,[19] and supported-Rh particles[8,20] as well.

Kinetic studies by Oh *et al.*[8] and Peden *et al.*[10] revealed that turnover frequencies of the CO oxidation at high pressures on rhodium single crystals and supported particles are very similar, indicating this reaction to be structure insensitive. However, under these conditions the surface is largely covered by CO and the rate is limited by the dissociative adsorption of oxygen. Kinetic studies at conditions where oxygen is the majority reactive intermediate, however, do reveal rates that depend on structure, as shown by Bowker *et al.* for Rh(111) and Rh(110).[11] Several authors report kinetic parameters for the CO oxidation on Rh(111), however, these values differ widely, e.g., from activation energies of 70 kJ/mol[13] to 190 kJ/mol.[4]

The kinetics of surface reactions under high coverage conditions, where lateral interactions cause adsorbates to order into islands and reactions may even occur in the oscillatory regime, has received considerable interest from experimentalists[3] and theoreticians[25] in the past decade. Recent scanning tunneling microscopy (STM) work by Wintterlin *et al.* points to the importance of reactive CO–O pairs at the boundaries between islands of adsorbed CO and O on Pt(111).[26] On rhodium, the reacting species O_{ads} and CO_{ads} may either segregate into separate phases,[4] or form mixed structures,[27,28] depending on coverages and on temperature.

Several studies demonstrate that different oxygen structures on rhodium surfaces possess different reactivity toward adsorbed CO,[15,16,29–31] whereas reconstruction has also been shown to affect the reactivity on Rh(110).[15] Baraldi *et al.*,[16] investigating the reaction between CO and preadsorbed oxygen on Rh(100), observed a higher reactivity for the reconstructed $(2\times2)p4g$ O-structure ($\theta_O = 0.50$ ML) than for the $p(2\times2)$-O structure ($\theta_O = 0.25$ ML).[32] The lower reactivity of the latter was explained by reduced mobility of CO, preventing it to overcome the barrier imposed by CO–O repulsion.

The strong dependence of mechanism and kinetics on adsorbate coverages is an important factor behind the large differences in activation energies and preexponential factors as reported in the literature. In fact, such parameters are only meaningful for elementary surface reactions in the limit of low coverages of at least one of the adsorbates.[33,34]

The purpose of this paper is to determine the kinetic parameters of the reaction between preadsorbed CO and O on Rh(100) and Rh(111) by means of temperature-programmed reaction spectrometry. The results confirm the structure sensitivity of the CO oxidation reaction, and demonstrate in a systematic way the effect of adsorbate coverages on the rate of the reaction.

a)Corresponding author: Phone: +31 40 247 3067, Fax: +31 40 245 5054, E-mail: J.W.Niemantsverdriet@tue.nl

II. EXPERIMENT

The experiments were done in two stainless steel ultrahigh vacuum systems with a base pressure of 10^{-10} mbar. The experiments with Rh(100) were done in a Leybold TPD/SIMS spectrometer equipped with a SSM 200 mass spectrometer system as previously described by Borg *et al.*[35] The experiments on Rh(111) were done in a home built UHV system, equipped with a Baltzers Prisma quadrupole mass spectrometer (QMA 200) and an Omicron LEED/Auger system, described in detail in a previous publication.[36] Some of the experiments with Rh(100) were repeated in the second system to verify that the temperature calibration in both systems was the same.

In both systems, the rhodium crystals of (100) and Rh(111) orientation with a thickness of about 1.2 mm were spotwelded on two tantalum wires of 0.3 mm diameter, pressed into small grooves on the side of the crystal. This construction allows for resistive heating up to 1450 K. The samples could be cooled to 100 K by flowing liquid nitrogen through the manipulator. Temperatures were measured with a chromel-alumel thermocouple spotwelded to the back of the crystal.

The Rh(100) crystal surface was cleaned by cycles of argon sputtering and annealing under oxygen and UHV, as described elsewhere.[37] The Rh(111) crystal surface was cleaned in a similar fashion at slightly higher temperatures, as described previously.[13] After the cleaning procedure, residual oxygen was removed and surface order was restored by annealing the crystals to 1400 K. Surface cleanliness and ordering were checked by Auger spectroscopy, which did not show any contamination and LEED, which showed sharp $p(1\times1)$ patterns for both crystals. Also, the absence of CO_2 during TPD of CO confirms the complete removal of residual oxygen on both crystals.

Oxidation of CO to CO_2 was studied by depositing a fixed amount of atomic O at 273 K after which the sample was cooled to 175 K or below to adsorb CO. Carbon monoxide (Hoek Loos, 99.995% pure) and oxygen (20% O_2/80% Ar) were used without further purification. The initial coverages of CO were determined from the amount of desorbing carbon atoms, by integrating the CO_2 and CO desorption peaks, dividing the CO peak area by the relative difference in mass spectrometer sensitivity for CO_2 and CO ($=1.1$), and adding these contributions. For the saturation coverage of CO on Rh(100) we used the value of 0.75 ML for the $p(4\sqrt{2}\times\sqrt{2})R45°-$CO/Rh(100) structure[36] and for CO on Rh(111) the value of 0.75 ML corresponding to the (2×2)-3CO/Rh(111) structure.[38,39] The CO TPD spectra were corrected for cracking of CO_2 in the mass spectrometer. The amount of preadsorbed oxygen on Rh(100) was determined from the amount of CO_2 formed in TPD, since the removal of O_{ads} appeared to be complete in the presence of an equal or higher amount of CO. On Rh(111) removal of O_{ads} is not always complete, so the amount of oxygen was determined from O_2-TPD, using the saturation coverage of 0.50 ML for O on Rh(111).[27,40,41] All TPD spectra were taken at a heating rate $\beta=5$ K/s.

Kinetic parameters for the reaction between CO and O were determined on the assumption that the reaction is, at least at low coverages, first-order in adsorbed O and CO, while CO_2 desorbs instantaneously. Provided both reactants are homogeneously distributed over the surface, the rate of CO oxidation r_{ox} is given by the following Arrhenius-equation:

$$r_{ox}=\upsilon\times\theta_{CO}\times\theta_O\times\exp\left(-\frac{E_a}{RT}\right), \tag{1}$$

which can be rewritten

$$\ln\left(\frac{r_{ox}}{\theta_{CO}\times\theta_O}\right)=\ln\nu-\frac{E_a}{RT}. \tag{2}$$

The adsorbate coverages θ_{CO} and θ_O can be calculated at any temperature from the CO and CO_2 TPD spectra. A plot of $\ln(r_{ox}/(\theta_{CO}\times\theta_O)$ versus $1/T$ yields the activation energy E_a and the preexponential factor ν from the slope and the intercept, respectively.

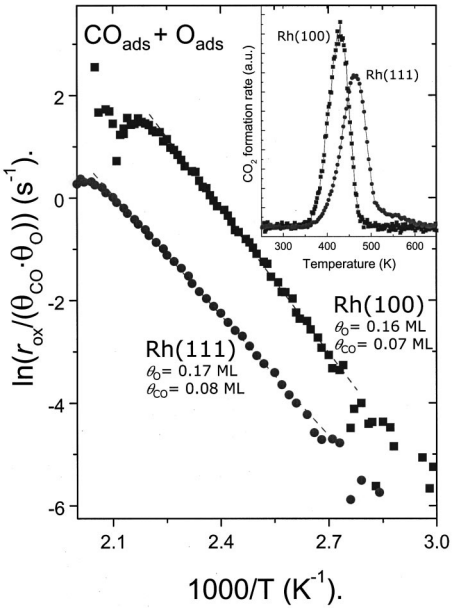

FIG. 1. Kinetic plots obtained from coverage-corrected leading edge analysis for CO oxidation on Rh(100) and Rh(111) at equal reactant coverages. Kinetic parameters can be derived by plotting the natural logarithm of the reaction rate constant ($r_{ox}/(\theta_{CO}\times\theta_O)$) vs reciprocal temperature. The activation energy E_a and preexponential factor ν can be determined from the slope ($-E_a/R$) and the intercept ($\ln(\nu)$), respectively. The inset shows the corresponding CO_2-TPD spectra for Rh(100) and Rh(111).

III. RESULTS

To illustrate the experimental approach and the kinetic analysis we compare the results of CO oxidation experiments at similar coverages on the two rhodium surfaces. Approximately 0.16 ML of O-atoms and 0.07 ML of CO were coadsorbed on each surface. The inset of Fig. 1 shows the TPD spectra of CO_2. The structure sensitivity of the reaction is evident from the significantly faster rate of reaction on Rh(100) than on Rh(111). A second difference between the two systems is that on Rh(100) all CO is oxidized to CO_2, whereas on Rh(111) part of the CO desorbs. The main part of Fig. 1 shows the Arrhenius plots according to Eqs. (1) and (2) over the entire temperature range of the TPD peaks. The

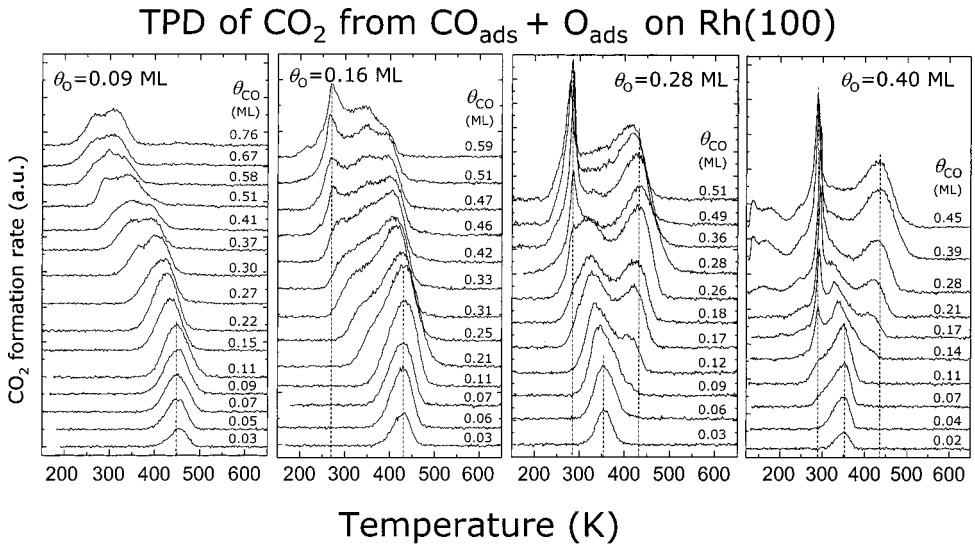

FIG. 2. CO_2 formation from different amounts of CO on oxygen-precovered Rh(100). Oxygen atoms were deposited by adsorbing a O_2/Ar gas mixture (20% O_2/80% Ar) at 273 K; a heating rate of 5 K/s was applied. Note that the desorption spectra at different O-precoverages have not been scaled with respect to each other .

fact that these lines are straight for a large temperature interval confirms that at these low coverages the reaction exhibits first-order kinetics with respect to both θ_O and θ_{CO}. Hence, the kinetic parameters can be derived with good accuracy. We will discuss the values of these parameters later on, when experiments at a large range of coverages have been described.

A. Oxidation of CO on Rh(100)

Figure 2 gives an overview of the temperature-programmed reactions between fixed amounts of preadsorbed oxygen (θ_O=0.09 ML, 0.16 ML, 0.28 ML, and 0.40 ML), and different amounts of CO from almost zero up to saturation coverage. At low coverages, CO_2 forms in a single peak. As the total coverage increases, several additional channels become available for oxidation. We discuss these later on.

Integration of the CO_2 and CO TPD spectra (not shown) yield the fractions of CO reacted to CO_2 as a function of initial CO coverage; see Fig. 3. Essentially, as long as O-atoms are available all CO is oxided on Rh(100). Only at higher oxygen coverages (θ_O=0.28 and 0.40 ML), some CO desorbs in parallel to CO_2, but also in this case the selectivity towards oxidation is high.

Kinetic analysis as explained in the experimental part was applied to those spectra which exhibit a single desorption state. Figure 4 gives an example of activation energies and preexponential factors obtained for the series of spectra at an oxygen precoverage of 0.09 ML. The peak shifts in the TPD spectra to lower temperatures with increasing CO coverage are reflected in a decrease of the activation energy and the preexponential factor. Also note that the change in slope around θ_{CO}=0.1 ML corresponds with the downward shift of the leading edge in the CO_2 TPD spectra (Fig. 2).

At θ_O=0.40 ML and low CO coverages, the oxygen coverage is much higher than that of CO, and the reaction becomes pseudo first order in CO. In this case we can also apply Chan-Aris-Weinberg (CAW1/2) analysis.[42] This yields

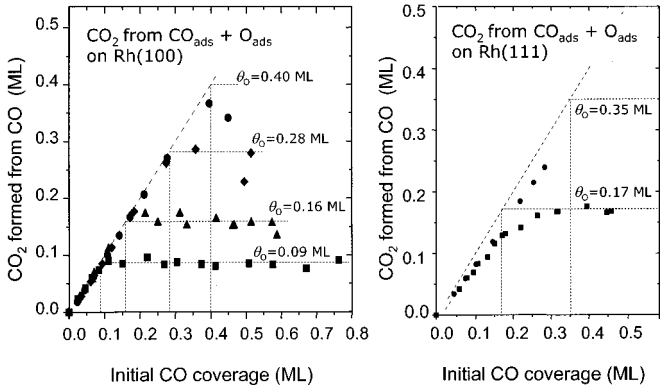

FIG. 3. Amount of CO_{ads} reacted with O_{ads} to CO_2 on Rh(100) (left) and Rh(100) (right), derived by integration of TPD spectra. The dotted lines are representative for the ideal case of stoichiometric reaction between CO_{ads} and O_{ads}.

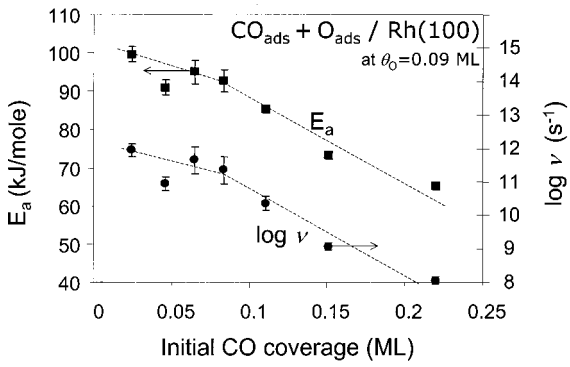

FIG. 4. Activation energy E_a (left axis) and preexponential factor ν (right axis) for CO oxidation on Rh(100) at θ_O=0.09 ML as a function of initial CO-coverage. Kinetic parameters were derived using coverage-corrected leading edge analysis as in Fig. 1. Dotted lines between experimental data points are drawn as a guide for the eye.

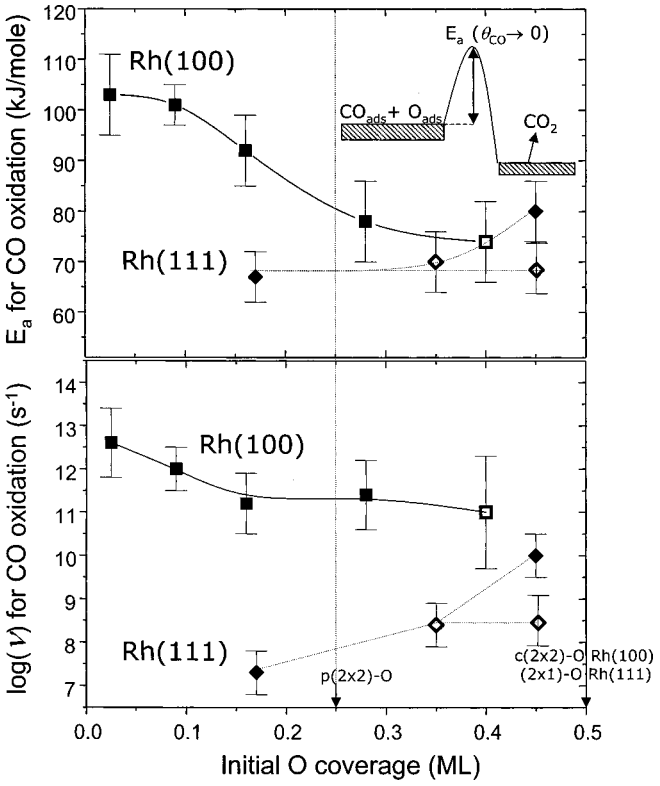

FIG. 5. Activation energy E_a (upper panel) and preexponential factor ν (lower panel) for CO oxidation on Rh(100) and Rh(111) in the limit of zero CO coverage, as a function of the amount of preadsorbed O. Datapoints, represented by filled symbols, were derived using coverage-corrected leading edge analysis and the open symbols using Chan–Aris–Weinberg analysis assuming zeroth order kinetics in θ_O and first-order kinetics in θ_{CO}. The dotted line at $\theta_O=0.25$ ML indicates the completion of the $p(2\times2)$-O structure. Solid lines between experimental data points are drawn as a guide for the eye.

an activation energy $E_a=74\pm8$ kJ/mol and a preexponential factor $\nu=10^{11\pm1.3}$ s^{-1} in the zero CO coverage limit. As a double check, we applied the Redhead formula[43] for $\nu=10^{11\pm1}$ s^{-1}, taking $T_{max}=350$ K and $\beta=5$ K/s, which yields an activation barrier $E_a=76\pm5$ kJ/mol, consistent with the CAW1/2 analysis.

The kinetic parameters obtained as in Fig. 4 were extrapolated to zero CO coverage for all four initial O-coverages; these extrapolated values are shown in Fig. 5. Both the activation energy and the preexponential factor for CO oxidation decrease with increasing O-coverage on Rh(100). The preexponential factors are all in accordance with the reaction $CO_{ads}+O_{ads}$ being an elementary step.[33,34]

B. Oxidation of CO on Rh(111)

The oxidation of CO on Rh(111) has been described extensively in the literature.[4–13] However, as the kinetic parameters reported vary considerably between different authors, we prefer to determine some kinetic data on this surface in the same manner as we did for Rh(100), to allow meaningful comparison.

Figure 6 shows the TPD spectra of CO_2 and CO for fixed amounts of 0.17 and 0.35 ML O coadsorbed with varying amounts of CO. The CO TPD spectra have been corrected for cracking of CO_2. At low coverages, CO_2 is formed between 400 and 500 K. At higher coverages, a faster CO_2 formation channel around 350 K becomes available, in good agreement with earlier observations.[4,27] This faster reaction channel is possibly associated with CO in a different binding geometry.[27,28] Also note the small upward temperature shift of the CO desorption with increasing θ_{CO} as more O-atoms are removed, decreasing the repulsion between CO_{ads} and O_{ads}. The amount of CO reacted to CO_2 has been included in Fig. 3 and the activation energies and preexponential factors for oxidation, derived in a similar way as for Rh(100), in Fig. 5.

Analyzing the spectra in terms of Eq. (2) was not successful for the spectra at high oxygen coverage of 0.35 ML, as the kinetic plots could not be fitted with straight lines. As for low initial CO coverages the coverage of oxygen decreases only slightly during CO_2 formation, the reaction follows pseudo first-order kinetics in θ_{CO}. This allows for the application of Chan-Aris-Weinberg (CAW1/2) analysis, which yields an activation energy $E_a=70\pm6$ kJ/mol and a preexponential factor $\theta=10^{8.4\pm0.5}$ s^{-1} for CO oxidation in the limit of zero CO coverage. These values are confirmed by Redhead analysis, which yields $E_a=72$ kJ/mol, assuming $\nu=10^{8.4}$ s^{-1} ($T_{max}=425$ K, $\beta=5$ K/s). This value is included in Fig. 5.

We also considered CO_2 formation for θ_O close to the saturation value of 0.50 ML, where O-atoms are reported to form a 3-domain (2×1)-structure with O-atoms in rows separated by one Rh-lattice constant.[27,40,41] The uptake of CO is limited to only 0.03 ML of CO at saturation. Interestingly, recent high-resolution core-electron spectroscopy measurements by Jaworowski *et al.*[28] point to the existence of an ordered 2O+CO phase with $\theta_O=0.50$ ML and $\theta_{CO}=0.25$ ML, which we have not been able to realize. At these very high O/CO ratios, oxidation is complete as CO desorption is hardly observed. Formation of CO_2 occurs in a single state around 410 K, not shifting with θ_{CO}. Analysis by Eq. (2) yields an activation energy of 80 ± 6 kJ/mol and a preexponential factor of $10^{10\pm0.5}$ s^{-1} for CO oxidation in the zero CO coverage limit. As the CO oxidation becomes first-order in θ_{CO} under these conditions, Chan–Aris–Weinberg analysis becomes applicable again, which yields the lower values of $E_a=69\pm5$ kJ/mol and $\nu=10^{8.5\pm0.5}$ s^{-1}.

As the spectra in Fig. 6 and the quantification in Fig. 3 show, oxidation of CO is accompanied by desorption of CO at all coverages. This desorption is at lower temperatures than observed for CO on oxygen-free Rh(111). At comparable coverages of O and CO, the peak temperatures for oxidation on Rh(111) are at least 35 K higher than on Rh(100). At high coverages, the difference becomes even larger. As a result, the oxidation reaction on Rh(111) falls largely in the temperature range where CO desorption occurs as well, and the selectivity for CO_2 formation is significantly lower on Rh(111) than on Rh(100).

The kinetic parameters for CO oxidation on Rh(111) are completely different than those for comparable CO- and O-coverages on Rh(100). The preexponential factors for CO oxidation on Rh(111) are in the range of 10^7-10^9 s^{-1}, which is lower than normally observed for an elementary

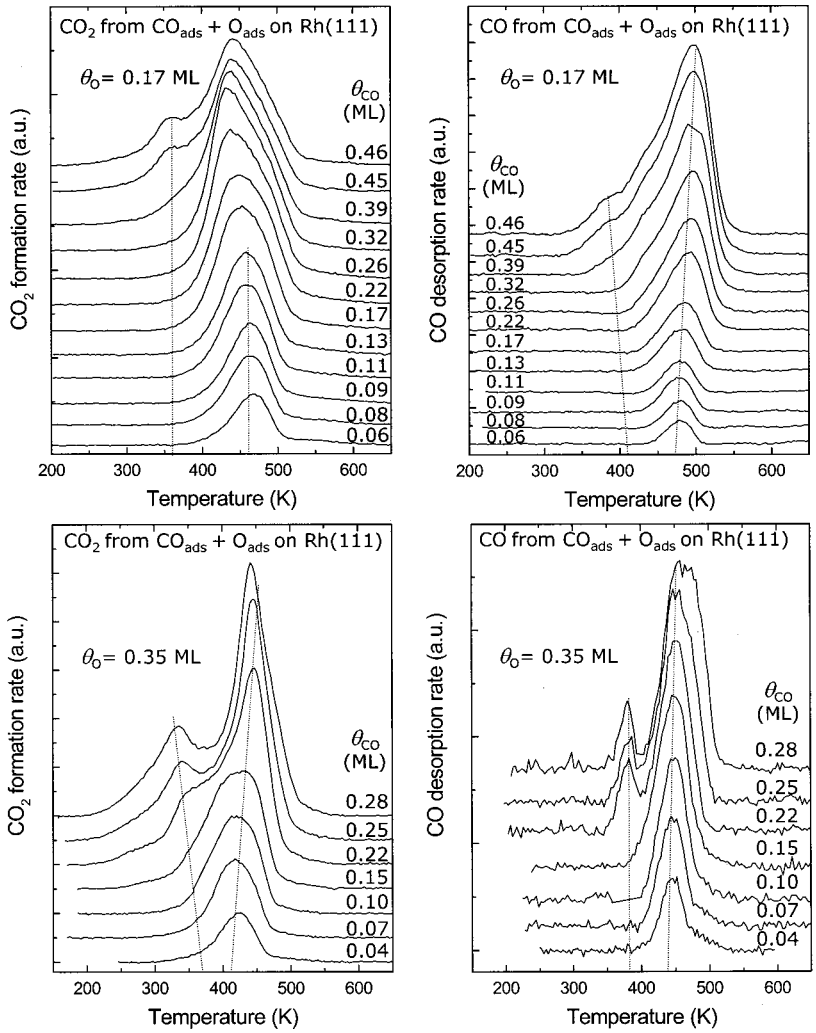

FIG. 6. TPRS spectra of CO_2 (left) and CO (right), for a fixed amount of 0.16 ML O (top) and 0.35 ML (bottom) coadsorbed with varying amounts of CO ($T_{ads}<175$ K). Oxygen atoms were deposited by adsorbing a O_2/N_2 gas mixture (20%/80%) at 293 K and a heating rate of 5 K/s was applied. CO-TPD spectra have been corrected for cracking of CO_2.

step. This may indicate that CO oxidation on Rh(111) cannot be described by a simple mean-field Langmuir–Hinshelwood approach, as we discuss further on.

Finally, Fig. 7 shows the uptake of CO on O-precovered Rh(100) and Rh(111) surfaces. On Rh(100) O-atoms and CO molecules are mutually exclusive with respect to adsorption sites, despite the fact that CO and O are adsorbed in different sites, as the sum of θ_O and θ_{CO} is constant ($\approx$0.82 ML). However, on Rh(111) the sum of the coverages decreases significantly when the surface fills up. When the rhodium surfaces are close to saturation with O-atoms, Rh(100) can still accommodate a stoichiometric amount of CO, whereas on Rh(111) hardly any CO can be chemisorbed.

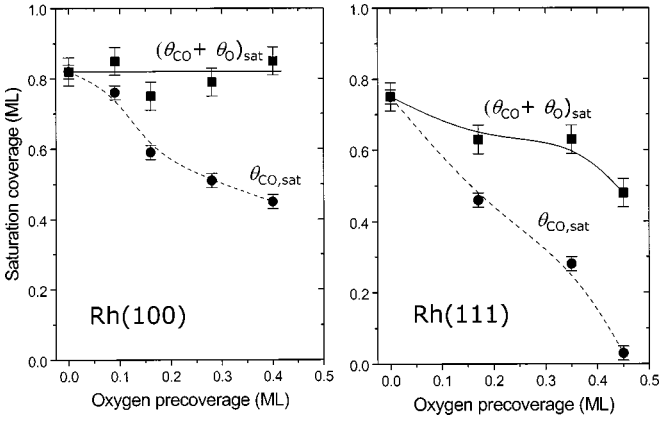

FIG. 7. Effect of O-precoverage on the total saturation coverage $(\theta_O + \theta_{CO})_{sat}$ and the CO saturation coverage $\theta_{CO,sat}$ on Rh(100) and Rh(111). Whereas on Rh(100) the total coverage is hardly affected over the whole coverage range, less CO can be accommodated within the O-structure at higher O-coverage on Rh(111).

IV. DISCUSSION

A. Structure sensitivity of the CO oxidation on rhodium

The direct comparison of the rate constant for CO oxidation over Rh(100) and Rh(100) in Fig. 1, as well as the difference in kinetic parameters at different oxygen coverages collected in Fig. 5, clearly illustrate the structure sensitivity of the CO oxidation reaction in the regime where reactant coverages are low. As stated in the Introduction, the reaction becomes apparently insensitive for catalyst structure under conditions where CO is the majority reacting intermediate, i.e., under steady state conditions for CO and O_2 partial pressures ranging from 1 to ~100 mbar at relatively low temperatures (~500 K). Under these conditions, the CO_2 formation exhibits first-order in the partial pressure of O_2 and

negative first-order in CO.[10] Here the reaction is rate-limited by the availability of dissociatively adsorbed oxygen. Hence, under these conditions desorption of CO is required to liberate empty sites for dissociation of O_2. Comparison of CO desorption from Rh(111),[44] Rh(110),[11,45] Rh(100),[16,36] and supported Rh-particles[46] shows that the rates of CO desorption are quite similar on these surfaces. So it appears that, instead of CO oxidation, desorption of CO is structure insensitive. Only weak dependence of the adsorption energy on surface structure of a molecular adsorbate like CO is in line with theory predictions.[33,47] This probably explains the very similar reaction rates, observed under high-pressure steady state experiments. This is the regime investigation by Goodman,[6] Oh,[8] and Peden and co-workers.[10] Bowker *et al.* studied the reaction under steady state conditions as a function of temperature on both Rh(111) and Rh(110).[11] He observed that the rates were similar at low temperature, but different at high temperature, in full agreement with the notion that CO_{ads} dominates the surfaces at lower and O_{ads} at higher temperatures. A similar conclusion can be drawn from the experiments by Schwartz *et al.* for CO oxidation on Rh(111) and Rh(100).[7] For temperatures higher than 600 K, the CO_2 formation rate on Rh(100) was found to be higher by one order of magnitude than on Rh(111), at comparable reactant pressures.

The major differences between the two rhodium surfaces with respect to CO oxidation investigated here are:

• At relatively low O-coverage the rate on Rh(100) is roughly an order of magnitude faster than on Rh(111). Structure dependence becomes even more pronounced at higher O-coverage, as the rate on Rh(100) becomes about 10^2 faster than on Rh(111).

• As long as O-atoms are available, all CO oxidizes to CO_2 on Rh(100); on Rh(111) CO desorption competes with oxidation, as the rate of CO oxidation is comparable to CO desorption on Rh(111). This is demonstrated in Fig. 8. We exclude (partial) migration of O_{ads} into subsurface sites on Rh(111) as the cause for this lowered selectivity to CO_2. A recent X-ray Photoemission Diffraction (XPD) study by Wider *et al.*[48] shows that subsurface sites only become occupied at elevated temperature and high O_2 exposures, i.e., when θ_O exceeds 0.50 ML.

• CO oxidation on Rh(100) exhibits kinetic parameters ($E_a = 103 \pm 5$ kJ/mol, $\nu = 10^{12.7 \pm 0.7}$ s^{-1} at $\theta_O = \theta_{CO} \rightarrow 0$) representative of a true elementary step, whereas the CO oxidation on Rh(111) is characterized by kinetic parameters ($E_a = 65 \pm 5$ kJ/mol; $\nu = 10^{7.5 \pm 1}$ s^{-1} at $\theta_O = 0.16$ ML; $\theta_{CO} \rightarrow 0$) indicative for a more complicated reaction sequence.

The total coverage of O and CO, achieved when CO is adsorbed to saturation on O-precovered surfaces is significantly larger on Rh(100) than on Rh(111), as shown in Fig. 7. Whereas the sum $\theta_O + \theta_{CO}$ is approximately constant and equal to 0.82 ML on Rh(100), the total coverage decreases in monotonous fashion from 0.75 ML for fully saturated CO/Rh(111) to 0.5 ML for fully saturated O/Rh(111). Apparently, no CO molecules can be accommodated within the (2×1)-O structure on Rh(111). This is consistent with the observation of inhibition in the CO_2 formation on Rh(111) for high oxygen coverage, at higher temperature and high $p(O_2)/p(CO)$ ratio.[7,10] The fact that CO oxidation is faster on Rh(100) than on Rh(111) is somewhat surprising. In view of the higher heat of adsorption of atoms on more open surfaces, while the heat of adsorption of CO on different surfaces of rhodium is not too different, one might have expected the rate of reaction to be slower on the (100) surface. The fact that this is not so many have to do with differences in the activated complex or transition state for CO_2 formation, on which information for the case on rhodium is not available, however. In the transition state for CO oxidation on the closest-packed surfaces of Pt and Ru it appears that partial loosening of the oxygen–metal bond gives the highest contribution to the reaction energy barrier.[49–51] It is well possible that this step is energetically more favorable on the (100) surface, owing to the different geometry on the more open surface.

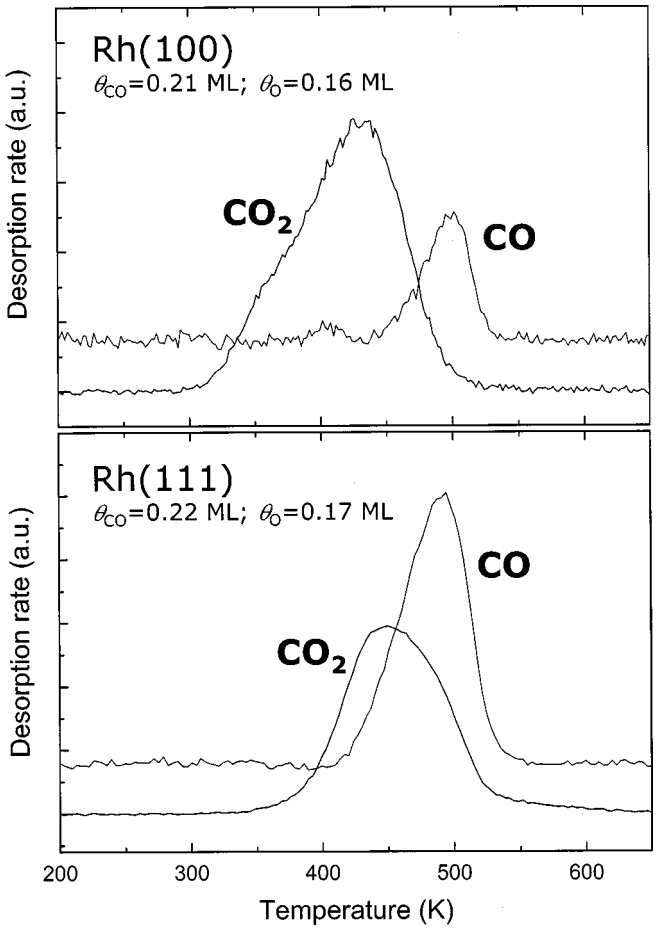

FIG. 8. Selected CO_2 and CO desorption traces from Figs. 2 and 6 for equal reactant coverages on Rh(100) and Rh(111). Clearly CO_2 formation goes to completion on Rh(100) as only a small excess of CO is seen to desorb, whereas on Rh(111) desorption and oxidation of CO are competing processes.

B. Different CO_2 formation channels on Rh(110)

The overview of temperature-programmed CO_2 formation from CO_{ads} and O_{ads} at different initial coverages in Fig. 2 reveals several reaction channels. At low coverages of both CO_{ads} and O_{ads}, CO_2 forms in a single peak around 450 K. Analyzing this in terms of the straightforward rate equation

(2), which expresses first-order kinetics in each reactant, yields $E_a = 103 \pm 7$ kJ/mol and $\nu = 10^{12.7 \pm 0.7}$ s^{-1}. In particular the preexponential has a value characteristic for an elementary step[33,34] and hence, it appears reasonable to attribute the CO_2 reaction channel at 450 K to a reaction between species that are randomly distributed across the surface and encounter each other because at least one the reactants, in this case CO, diffuses freely over the surface. A previous Monte Carlo simulation of ordering phenomena of NO on Rh(111) indicated that diffusion of molecules such as NO and CO started to become detectable at much lower temperatures of 200 K already, and that diffusion of these molecules was by far the fastest surface process at temperatures above 250 K.[52] Adsorbed atoms diffuse much more slowly, although mobility of O-atoms on ruthenium at room temperature has been demonstrated.[53]

Considering reaction around 450 K as the reference case for the limit of low reactant coverage, we see that increasing the precoverage of O-atoms but keeping the CO coverage low (below about 0.10 ML) leads to an intrinsically faster reaction, characterized by a lower activation energy, and a preexponential factor that changes only insignificantly (Fig. 5). The reason that the reaction goes faster with increasing number of oxygen atoms in the low coverage regime ($\theta_O < 0.25$ ML) is probably that the O-atoms enhance the electrostatic potential of the surface with a long range effect that is similar but opposite in sign as small amounts of alkali do.[54] As a result the CO becomes destabilized on the entire surface. This leads to enhanced mobility and, probably also, reactivity toward O.

In the high coverage regime ($\theta_O > 0.25$ ML) the reaction rate is probably increased due to repulsive interactions between O-atoms, as evidenced both from TPD,[55] single crystal adsorption calorimetry (SCAC),[56] and density functional theory (DFT) calculations.[57,58] This leads to a decrease in the oxygen binding energy and hence a lower reaction barrier for CO oxidation. DFT calculations for CO oxidation on noble metal surfaces reveal that the most important part of the energy barrier for CO oxidation is caused by partially loosening the O-atom in the transition state for CO_2 formation.[49–51] This also explains the observed trend in increasing activity for CO oxidation going from left (Ru) to right (Pd) in the periodic table, concomitant with the decrease in the oxygen binding energy.

Oxygen atoms are known to order on Rh(100) and this strongly affects the $CO_{ads} + O_{ads}$ reaction at higher coverages, as evidenced by Fig. 2. We propose the structural model of Fig. 9 to explain some of the observed shifts in the CO_2 formation. For oxygen coverages below 0.25 ML, the O_{ads}-atoms arrange in islands of $p(2\times2)$ geometry.[59] The first CO molecules will adsorb on the free metal patches, as CO prefers to bind linearly, as has been observed experimentally.[36] When the free metal is filled, additional CO has to penetrate the O-islands. According to Fig. 7, this is well possible on the Rh(100) surface. However, for O_{ads} coverages above 0.25 ML, the atoms in excess of 0.25 ML occupy centered positions in the (2×2) cell and at $\theta_O = 0.5$ ML the $c(2\times2)$ structure is complete.[59] Figure 9 indicates

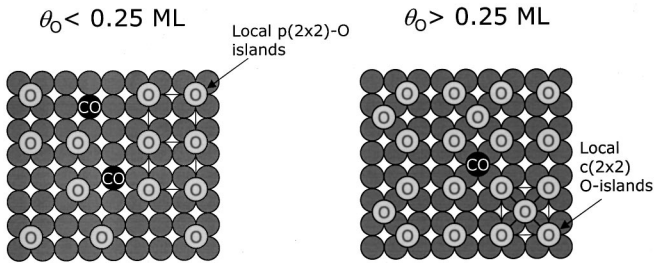

FIG. 9. Structural model for the CO oxidation on Rh(100) for initial O-coverages below 0.25 ML (left) and above (right) and low θ_{CO}. For $\theta_O < 0.25$ ML, O-atoms are arranged in local $p(2\times2)$-islands and the first CO molecules are probably linearly adsorbed on the bare metal patches, giving rise to CO_2 formation between 425 and 450 K. Upon completion of the ordered $p(2\times2)$-O ($\theta_O > 0.25$ ML) structure on Rh(100), excess O-atoms are arranged in local $c(2\times2)$-islands and the first CO molecules are adsorbed in a higher bonding geometry in close proximity to O_{ads}. This gives rise to CO_2 formation around 350 K.

that such surfaces can still accommodate about 0.25 ML of CO.

These considerations suggest we have the following reaction channels for O_{ads} and CO_{ads} on Rh(100):

• Low coverage of O_{ads} and CO_{ads}: Reaction between isolated species, characterized by a CO_2 formation peak around 450 K.

• $\theta_O < 0.25$ ML: O_{ads} present locally in $p(2\times2)$ islands, reaction of CO adsorbed initially adsorbed on free rhodium with O-atoms at the perimeter of these islands, CO_2 formation between 400 and 450 K. At higher CO coverages, reaction within the islands, between 300 and 400 K.

• $\theta_O > 0.25$ ML: O_{ads} present in a complete $p(2\times2)$ structure, with locally a $c(2\times2)$ structure. At low CO coverage all CO_{ads} is inside the $p(2\times2)$ and reacts to CO_2 between 300 and 400 K. At higher coverages of CO_{ads} reaction occurs in the $c(2\times2)$, with a sharp CO_2 formation peak at 280 K. We wonder if this peak is associated with the lifting of the well-documented clockwise–anticlockwise reconstruction of the Rh(100) surface upon saturation with O.[32,60–62]

The splitting up of the 350 K CO_2 formation into a lower and a higher temperature CO_2 formation channel with increasing CO coverage as seen in the right part of Fig. 2 is due to depletion of oxygen atoms. As θ_O decreases below the critical coverage of 0.25 ML, CO molecules will segregate to the bare metal patches, in-between the (2×2)-O islands and hence reaction proceeds in the lower reactivity channels.

C. Kinetic parameters CO oxidation

Kinetic parameters for CO oxidation on different rhodium surfaces as measured by various researchers are presented in Table I. As we have stated before, there is large scatter in the kinetic data for Rh(111). This can partly be explained by different reaction conditions. Under high pressure conditions, when the surface is almost completely covered by CO and the rate is limited by the availability of O, the activation energy amounts to ca. 110 kJ/mol.[6–8,10] Importantly, the preexponential factor is 10^{12} s^{-1} in all cases, suggesting that this is indeed an elementary step. These kinetic

TABLE I. Kinetic parameters for CO oxidation on Rh-surfaces.

Surface	Method	E_a (kJ/mol)	ν (s^{-1})	Conditions	Ref.
Rh(111)	UHV conditions, TPD (leading edge)	65±5 80±6	$10^{7.5\pm1}$ $10^{10\pm0.5}$	Low θ_O; low θ_{CO} High θ_O; low θ_{CO}	This work
	UHV conditions Molecular beam reactive scattering	102±2	$10^{12.3\pm0.3}$	High θ_O; low θ_{CO}	9
	10–300 mbar, steady state CO_2 production	106	10^{12}	Low θ_O; high θ_{CO}	6, 10
	10–300 mbar, steady state CO_2 productions	84±8	-	$T<425$ K	7
	UHV conditions, TPD (isostere analysis)	188 117	- -	Low θ_O; low θ_{CO} High θ_O; low θ_{CO}	4
Rh(111) Rh/Al_2O_3	10–300 mbar, steady state CO_2 production	121 126	10^{12} 10^{12}	Low θ_O; high θ_{CO} Low θ_O; high θ_{CO}	8
Rh-wire	Kinetic modeling	60 105	$10^{5.6}$ $10^{10.9}$	High θ_O; low θ_{CO} Low θ_O; high θ_{CO}	19
Rh(110)	Molecular beam Kinetic modeling	71	10^{7}	Low θ_O; high θ_{CO}	14
Rh(100)	UHV conditions, TPD (leading edge)	103±5 75±8	$10^{12.7\pm0.7}$ $10^{11\pm1.2}$	Low θ_O; high θ_{CO} High θ_O; low θ_{CO}	This work

parameters most probably reflect the kinetics of CO desorption from a CO-saturated surface as this frees up empty sites, necessary for the adsorption of oxygen. Steady-state experiments consider the overall reaction mechanism $CO_g + O_{2,g} \rightarrow CO_{2,g}$, and thus they are not very informative with respect to surface reaction step $CO_{ads} + O_{ads} \rightarrow CO_{2,g} + 2*$. TPD experiments only reflect the latter step, as the reactants are preadsorbed. Our experiments indicate that oxidation of CO in the low coverage limit on Rh(100) is an elementary step, whereas on Rh(111) it is not. This is most probably due to a nonhomogeneous distribution of the adsorbates on Rh(111). Mixed structures of CO and O on Rh(111) are only observed when the O-atoms are well-ordered.[27,28] However, in the absence of a well ordered O-overlayer, segregation of the reactants in islands is reported.[4] This implies that CO oxidation on Rh(111) cannot be described by the simple Arrhenius-equation (1), as reaction only occurs along the island perimeters. Surprisingly, this does not seem to occur on the more open Rh(100) surface, although formation of O-islands has been reported.[59] Surface structure might play a decisive role in this issue, as the absolute atom-density on Rh(100) is lower. This would imply that the oxygen structures on Rh(100) are more open than on Rh(111) at equal coverage. Possibly, this enables CO to penetrate more easily within the oxygen structures on Rh(100), whereas restricted mobility of CO on Rh(111) prevents CO to mix within O-islands. This is in agreement with Fig. 7.

We cannot, however, rule out that the CO oxidation on Rh(111) is dominated by steps as recently was found to be the case for the dissociation of N_2 on Ru(0001).[63] This would also lead to a low value of the preexponential factor, and it might also provide a good explanation for why the activation energy is apparently lower on Rh(111) than on Rh(100).

V. CONCLUSIONS

We have used Temperature-Programmed Reaction Spectroscopy to monitor the reaction between CO_{ads} and O_{ads} on two different Rh-surfaces, (100) and (111). We find that application of coverage-corrected leading-edge analysis, i.e., plotting the natural logarithm of the desorption rate divided by the actual coverages of the reactants versus $1/T$, works remarkably well to analyze the TPD spectra and to determine the kinetic parameters. The main results from this work are:

• Oxidation of CO on rhodium surfaces is a structure sensitive reaction. The surface reaction step $CO_{ads} + O_{ads} \rightarrow CO_{2,g}$ is intrinsically faster on Rh(100) than on Rh(111).

• As a consequence, selectivity to CO_2 is generally higher on Rh(100). On Rh(100) reaction between CO_{ads} and O_{ads} goes to completion, whereas on Rh(111) oxidation and desorption of CO are competing channels.

• At low CO coverage, CO oxidation is an elementary step on Rh(100) for a broad range of oxygen coverages. We report kinetic parameters $E_a = 103 \pm 5$ kJ/mol and $\nu = 10^{12.7\pm0.7}$ for $\theta_O = \theta_{CO} \rightarrow 0$.

• The activation energy for CO oxidation on Rh(100) continuously decreases with increasing O-coverage. At low coverage ($\theta_O < 0.25$ ML) we attribute this to destabilization of CO, leading to an increase in the CO_2 formation rate. At higher coverage ($\theta_O > 0.25$ ML) O-atoms become destabi-

lized as well, as lateral interactions between O-atoms come into play at these coverages.

• On Rh(100) the coverages of O-atoms and CO molecules add up to a constant coverage of 0.82 ML at all O-precoverages. On Rh(111), however, O-atoms progressively exclude the adsorption of CO, such that the saturation coverages of CO decreases from 0.75 ML in the absence of O_{ads} to zero at an O-saturated surface ($\theta_O = 0.5$ ML).

ACKNOWLEDGMENTS

This work was financially supported by the Netherlands Organization for Scientific Research–Chemical Sciences (NWO–CW) and performed under the auspices of the Netherlands Institute of Catalysis Research (NIOK).

[1] J. L. Gland and E. B. Kollin, J. Chem. Phys. **78**, 963 (1983).
[2] C. T. Campbell, G. Ertl, H. Kuipers, and J. Segner, J. Chem. Phys. **73**, 5862 (1980).
[3] G. Ertl, Adv. Catal. **37**, 213 (1990).
[4] T. Matsushima, T. Matsui, and M. Hashimoto, J. Chem. Phys. **81**, 5151 (1984).
[5] T. W. Root, L. D. Schmidt, and G. B. Fisher, Surf. Sci. **150**, 173 (1985).
[6] D. W. Goodman and C. H. F. Peden, J. Phys. Chem. **90**, 4839 (1986).
[7] S. B. Schwartz, L. D. Schmidt, and G. B. Fisher, J. Phys. Chem. **90**, 6194 (1986).
[8] S. H. Oh, G. B. Fisher, J. E. Carpenter, and D. W. Goodman, J. Catal. **100**, 360 (1986).
[9] L. S. Brown and S. J. Sibener, J. Chem. Phys. **89**, 1163 (1988); **90**, 2807 (1989).
[10] C. H. F. Peden, D. W. Goodman, D. S. Blair, P. J. Berlowitz, G. B. Fisher, and S. H. Oh, J. Phys. Chem. **92**, 1563 (1988).
[11] M. Bowker, Q. Guo, Y. Li, and R. W. Joyner, Catal. Lett. **18**, 119 (1993).
[12] J. I. Colonell, K. D. Gibson, and S. J. Sibener, J. Chem. Phys. **103**, 6677 (1995).
[13] M. J. P. Hopstaken, W. J. H. van Gennip, and J. W. Niemantsverdriet, Surf. Sci. **433-435**, 69 (1999).
[14] M. Bowker, Q. Guo, and R. W. Joyner, Surf. Sci. **280**, 50 (1993).
[15] F. M. Leibsle, P. W. Murray, S. M. Francis, G. Thornton, and M. Bowker, Nature (London) **363**, 706 (1993).
[16] A. Baraldi, L. Gregoratti, G. Comelli, V. R. Dhanak, M. Kiskinova, and R. Rosei, Appl. Surf. Sci. **99**, 1 (1996).
[17] L. W. H. Leung and D. W. Goodman, Catal. Lett. **5**, 353 (1990).
[18] B. A. Gurney, L. J. Richter, J. S. Villarubia, and W. Ho, J. Chem. Phys. **87**, 6710 (1987).
[19] C. T. Campbell, S.-K. Shi, and J. M. White, J. Phys. Chem. **83**, 2255 (1979).
[20] T. Bunluesin, H. Cordatos, and R. J. Gorte, J. Catal. **157**, 222 (1995).
[21] G. Ertl, Adv. Catal. **28**, 2 (1979).
[22] T. Matsushima and H. Asada, J. Chem. Phys. **85**, 1658 (1986).
[23] I. Z. Jones, R. A. Bennett, and M. Bowker, Surf. Sci. **439**, 235 (1999).
[24] A. Böttcher, H. Niehus, S. Schwegmann, H. Over, and G. Ertl, J. Phys. Chem. B **101**, 11185 (1997).
[25] R. J. Gelten, A. P. J. Jansen, R. A. van Santen, J. J. Lukkien, J. P. L. Segers, and P. A. J. Hilbers, J. Chem. Phys. **108**, 5921 (1998).
[26] J. Wintterlin, S. Völkening, T. V. W. Janssens, T. Zambelli, and G. Ertl, Science **278**, 1931 (1997).
[27] S. Schwegmann, H. Over, V. DeRenzi, and G. Ertl, Surf. Sci. **375**, 91 (1997).
[28] A. J. Jaworowski, A. Beutler, F. Strisland, R. Nyholm, B. Setlik, D. Heskett, and J. N. Andersen, Surf. Sci. **431**, 33 (1999).
[29] G. Comelli, V. R. Dhanak, M. Kiskinova, N. Pangher, G. Paolucci, K. C. Prince, and R. Rosei, Surf. Sci. **260**, 7 (1992).
[30] G. Comelli, V. R. Dhanak, M. Kiskinova, G. Paolucci, K. C. Prince, and R. Rosei, Surf. Sci. **269/270**, 360 (1992).
[31] P. W. Murray, F. M. Leibsle, Y. Li, Q. Guo, M. Bowker, G. Thornton, V. R. Dhanak, K. C. Prince, and R. Rosei, Phys. Rev. B **47**, 12976 (1993).
[32] W. Oed, B. Dötsch, L. Hammer, K. Heinz, and K. Muller, Surf. Sci. **207**, 55 (1988).
[33] R. A. van Santen and J. W. Niemantsverdriet, *Chemical Kinetics and Catalysis* (Plenum, New York, 1995).
[34] V. P. Zhdanov, Surf. Sci. Rep. **12**, 183 (1991).
[35] H. J. Borg, J. P. C.-J. M. Reijerse, R. A. van Santen, and J. W. Niemantsverdriet, J. Phys. Chem. **101**, 10052 (1994).
[36] A. M. de Jong and J. W. Niemantsverdriet, J. Phys. Chem. **101**, 10126 (1994).
[37] M. J. P. Hopstaken and J. M. Niemantsverdriet, J. Phys. Chem. B **104**, 3058 (2000).
[38] A. Beutler, E. Lundgren, R. Nyholm, J. N. Andersen, B. Setlik, and D. Heskett, Surf. Sci. **371**, 381 (1997).
[39] M. Gierer, A. Barbieri, M. A. van Hove, and G. A. Somorjai, Surf. Sci. **391**, 176 (1997).
[40] D. G. Castner and G. A. Somorjai, Appl. Surf. Sci. **6**, 29 (1980).
[41] K. C. Wong, W. Liu, and K. A. R. Mitchell, Surf. Sci. **360**, 137 (1996).
[42] C.-M. Chan, R. Aris, and W. H. Weinberg, Appl. Surf. Sci. **1**, 360 (1978).
[43] P. A. Redhead, Vacuum **12**, 203 (1962).
[44] P. A. Thiel, E. D. Williams, J. T. Yates, Jr., and W. H. Weinberg, Surf. Sci. **84**, 54 (1979).
[45] M. Bowker, Q. Guo, and R. W. Joyner, Surf. Sci. **253**, 33 (1991).
[46] V. Nehasil, S. Zafeiratos, S. Ladas, and V. Matolín, Surf. Sci. **433-435**, 215 (1999).
[47] B. Hammer, L. B. Hansen, and J. K. Nørskov, Phys. Rev. B **59**, 7413 (1999).
[48] J. Wider, T. Greber, E. Wetli, T. J. Kreutz, P. Schwaller, and J. Osterwalder, Surf. Sci. **417**, 301 (1998).
[49] A. Eichler and J. Hafner, Surf. Sci. **433-435**, 58 (1999).
[50] C. Stampfl and M. Scheffler, Surf. Sci. **433-435**, 119 (1999).
[51] A. Alavi, P. Hu, T. Deutsch, P. L. Silvestrelli, and J. Hütter, Phys. Rev. Lett. **80**, 3650 (1998).
[52] R. M. van Hardeveld, M. J. P. Hopstaken, J. J. Lukkien, P. A. J. Hilbers, A. P. J. Jansen, R. A. van Santen, and J. W. Niemantsverdriet, Chem. Phys. Lett. **302**, 98 (1999).
[53] J. Wintterlin, J. Trost, S. Renisch, R. Schuster, T. Zambelli, and G. Ertl, Surf. Sci. **394**, 159 (1997).
[54] T. V. W. Janssens, G. R. Castro, K. Wandelt, and J. W. Niemantsverdriet, Phys. Rev. B **49**, 14599 (1994).
[55] G. B. Fisher and S. J. Schmieg, J. Vac. Sci. Technol. A **1**, 1064 (1983).
[56] R. Kose, W. A. Brown, and D. A. King, Surf. Sci. **402-404**, 856 (1998).
[57] D. Loffreda, D. Simon, and P. Sautet, J. Chem. Phys. **108**, 6447 (1998).
[58] E. Hansen and M. Neurock, Surf. Sci. **441**, 410 (1999).
[59] A. Baraldi, V. R. Dhanak, G. Comelli, K. Prince, and R. Rosei, Phys. Rev. B **56**, 10511 (1997).
[60] D. Alfé, S. de Gironcoli, and S. Baroni, Surf. Sci. **410**, 151 (1998).
[61] A. Baraldi, J. Cerdá, J. A. Martin Gago, G. Comelli, S. Lizzit, G. Paolucci, and R. Rosei, Phys. Rev. Lett. **82**, 4874 (1999).
[62] J. R. Mercer, P. Finetti, F. M. Leibsle, R. McGrath, V. R. Dhanak, A. Baraldi, K. C. Prince, and R. Rosei, Surf. Sci. **352-354**, 173 (1996).
[63] S. Dahl, A. Logadottir, R. C. Egeberg, J. H. Larsen, I. Chorkendorff, E. Törnqvist, and J. K. Nørskov, Phys. Rev. Lett. **83**, 1814 (1999).